Acoustic propagation in a vortical homentropic flow

Jean-François Mercier, Colin Mietka, Florence Millot, Vincent Pagneux

ACOUSTIC PROPAGATION IN A VORTICAL HOMENTROPIC FLOW*

J-F. MERCIER†, C. MIETKA‡, F. MILLOT‡ , AND V. PAGNEUX§

Abstract. This paper is devoted to the theoretical and the numerical studies of the radiation of an acoustic source in a general homentropic flow. As a linearized model, we consider Goldstein's Equations, which extend the usual potential model to vortical flows. The equivalence between Linearized Euler's Equations with general source terms and Goldstein's Equations is established, and the relations between unknowns, in each model, are analysed. A closed-form relation between the hydrodynamic phenomena and the acoustics is derived. Finally, numerical results are presented and the relevance of using Goldstein's Equations compared to the potential model is illustrated.

Key words. Acoustics, Hydrodynamics, Goldstein's Equations, Finite Element Method, Discontinuous Galerkin Element Method, Perfectly Matched Layers

AMS subject classifications. 65J10, 65N30, 65Z05,35J50, 35Q35, 35Q31

1. Introduction.

Aeroacoustics consists in determining the acoustic perturbations propagating in an imposed flow. It is mostly the need of noise reduction in aeronautics which creates an increasing interest in the field of aeroacoustics, the main application concerning the sound propagation inside the radiation and outside a plane engine. But let us cite also the need to reduce the sound emitted by exhaust pipes in the car industry or by ventilation ducts in the domestic industry. In the present paper, we focus on the propagation of the sound created by a known source in a given flow. In particular we do not address the mechanisms responsible of noise generation [1, 2], involving non-linear models. We consider linearized equations and we focus on the time harmonic regime.

The most studied case of acoustic propagation in a flow is the case of a curl free carying flow. This case is simpler because for a uniform flow [3] or even for a flow $\mathbf{v}_0$ potential and homentropic, the acoustic perturbations are also potential and the velocity potential φ satisfies the convected Helmholtz equation [4, 5]:

$$\frac{\mathrm{D}}{\mathrm{D}t}\left(\frac{1}{c_0^2}\frac{\mathrm{D}\varphi}{\mathrm{D}t}\right) = \frac{1}{\rho_0}\mathrm{div}(\rho_0 \boldsymbol{\nabla}\varphi), \tag{1}$$

where ρ_0 and c_0 are respectively the density and the sound velocity of the flow and where

$$\frac{\mathrm{D}}{\mathrm{D}t} = \frac{\partial}{\partial t} + \mathbf{v}_0 \cdot \boldsymbol{\nabla}, \tag{2}$$

is the convective derivative. This model is well adapted to a classical Finite Element discretization and is widely used in some industrial applications [6, 7] or in the analysis of the influence of liners on the acoustic propagation [8, 9, 10].

For a more complex flow, a scalar description of acoustic perturbations is no longer possible because of the coupling between acoustic and hydrodynamic phenomena. Such coupling requires more sophisticated vector models. For the time-domain

*This work was funded by the Fog Research Institute under contract no. FRI-454.

†POEMS, CNRS-INRIA-ENSTA UMR 7231, 828 Boulevard des Maréchaux, 91762 Palaiseau, France (jean-francois.mercier@ensta-paristech.fr).

‡CERFACS, 42 avenue Gaspard Coriolis, 31057 Toulouse Cedex 01, France(colin.mietka@gmail.com, Florence.Millot@cerfacs.fr).

§LAUM CNRS UMR 6613, avenue O. Messiaen, 72085 Le Mans Cedex 9, France (Vincent.Pagneux@univ-lemans.fr).

problem, several methods have been developed to solve the Linearized Euler Equations, but the treatment of the artificial boundaries still raises open questions. On the other hand, the time-harmonic problem in an undounded domain has not been considered for a general flow, excepting thanks to the Galbrun equation [11]. However, the Galbrun equation [12, 13, 14] revealed not to be adapted to 3D configurations. To go beyond this limitation, in this paper we consider the Goldstein equations [15, 16]. They have been widely used to model the development of perturbations in a swirling flow [17, 18, 19, 20, 21, 22, 23] and we will show that they are well adapted for aeroacoustics applications.

The main advantage of using Goldstein's equations is that they are simpler than alternative models, among which the Linearized Euler equations [24, 25, 26, 27], the Galbrun equation or the Möhring equations [28, 29], because they are mainly scalar and close to a usual wave equation. Indeed, they can be seen as a perturbation of the simple convected Helmholtz equation (1) and they even exactly reduce to this equation in the potential areas of the carrier flow, this last point being particularly important for 3D applications.

In this paper, we study theoretically and numerically the radiation of general sources in a general flow, using the Goldstein equations. A general flow means a flow at least not potential, but also not only a parallel shear flow, for which Pridmore-Brown equation [30] is more commonly used. In addition to the velocity potential, Goldstein's equations involve a supplementary unknown, namely the hydrodynamic vector field $\boldsymbol{\xi}$, which satisfies a transport equation. Our main contribution is to determine the closed-form expression (14) of the Goldstein hydrodynamic unknown $\boldsymbol{\xi}$. In particular we will show that for a potential flow and potential sources, $\boldsymbol{\xi} = \mathbf{0}$ and Eq. (1) is recovered. Note that Goldstein derived his equations only in the case of a potential flow in presence of incident convected disturbances but without explicit source term (see Eq. (9)). Since we are interested in a general configuration, we derive the equations in the general case. Starting from Euler's equations, we first derive a generalization of the Goldstein equations that are valid in presence of compactly supported source terms and of a vortical flow as well. Finally, since the Goldstein equations are exact, we will quantify the errors when the convected Helmholtz equation (1) is used in a non potential flow, such approximation being often used for its simplicity.

The outline of the paper is the following. The generalized Goldstein equations are derived in section 2 and we show they are equivalent to Euler's equations. This section ends up with the determination of the general expression of $\boldsymbol{\xi}$. Section 3 is mainly devoted to some 2D numerical experiments. First, we consider a parallel shear flow in an unbounded domain. Such simple flow facilitates the presentation of the numerical method, based on the introduction of Perfectly Matched Layers (PMLs) to bound the calculation domain and on the coupling between continuous and discontinuous Finite Elements. We also give some conditions under which the radiation problem with PMLs is well-posed, ensuring the convergence of the Finite Element scheme. Then we use Goldstein's equations to study numerically the acoustic radiation of a source in presence of such a flow. The solutions are validated by comparison with the solutions obtained from the Galbrun equation and the influence of a vortical flow is illustrated. Finally we consider a non-parallel flow and we illustrate the closed-form relation giving $\boldsymbol{\xi}$.

2. Derivation of the Goldstein equations from the Euler equations.

Our first purpose is to prove in a simple and comprehensive way the equivalence between

Euler's equations and Goldstein's equations in presence of source terms and of a vortical flow. Although we are primary interested in the time harmonic regime, such proof will be done in the time regime because the initial conditions enable us to have uniqueness results when integrating transport equations. We start by recalling the Linearized Euler Equations.

2.1. Euler's equations. Since the theory is not limited to a 2D configuration, we work in 3D and we consider a propagation domain $\Omega = \mathbb{R}^3$ or $\Omega = \mathbb{R}^3 \backslash B$ where B represents obstacles or walls guide, on which a rigid boundary condition is imposed $\tilde{\mathbf{v}} \cdot \mathbf{n} = 0$ with $\tilde{\mathbf{v}}$ the total fluid velocity. We consider a subsonic inviscid flow of a perfect compressible fluid with constant specific heats capacity c_p and c_v at constant pressure and volume. The flow is the superposition of a steady flow and of small time-dependent acoustic perturbations: the velocity $\mathbf{v}$, the density ρ, the pressure p and the entropy s. The small perturbations satisfy in Ω the Linearized Euler Equations.

Following Goldstein [15], it is assumed that the carrier flow is homentropic: s_0 is constant. This is an hypothesis commonly used [17, 18, 19, 20], despite effects of a mean entropy have been sometimes taken into account [21, 22]. For such a carrier flow, Goldstein showed that the Linearized Euler Equations simplify in a system that we extend by including general source terms f, $\mathbf{g}$ and h:

$$\left\{ \begin{array}{l} \dfrac{D\mathbf{v}^\star}{Dt} + (\mathbf{v}^\star \cdot \boldsymbol{\nabla})\mathbf{v}_0 + \boldsymbol{\nabla}\left(\dfrac{p}{\rho_0}\right) = \mathbf{g}, \\ \dfrac{D}{Dt}\left(\dfrac{p}{\rho_0 c_0^2}\right) + \dfrac{1}{\rho_0}\mathrm{div}\,(\rho_0 \mathbf{v}) = -f, \\ \dfrac{Ds}{Dt} = h, \\ \mathbf{v}^\star = \mathbf{v} - \dfrac{s\mathbf{v}_0}{2c_p}. \end{array} \right. \tag{3}$$

$\mathrm{D}/\mathrm{D}t$ is defined in Eq. (2) and the boundary conditions are $\mathbf{v} \cdot \mathbf{n} = 0$ on $\partial\Omega$. Source terms are chosen compactly supported and such that $f, h \in L^2(\Omega)$, $\mathbf{g} \in (L^2(\Omega))^3$. We consider causal sources and null initial conditions:

$$\begin{aligned} &f(\mathbf{x}, t \leq 0) = 0 = \mathbf{g}(\mathbf{x}, t \leq 0) = h(\mathbf{x}, t \leq 0), \\ &\mathbf{v}^\star(\mathbf{x}, 0) = 0 = p(\mathbf{x}, 0) = s(\mathbf{x}, 0). \end{aligned}$$

In (3), the entropy perturbation s is decoupled from the other perturbations. Note that this is no longer true if the carrier flow is not homentropic. Then the entropy satisfies $\dfrac{Ds}{Dt} + \mathbf{v} \cdot \boldsymbol{\nabla} s_0 = h$ and as soon as $s_0 \neq 0$, s depends on $\mathbf{v}$. For a homentropic carrier flow, s can be eliminated by solving the following decoupled problem:

$$\left\{ \begin{array}{rcl} \dfrac{\mathrm{D}s}{\mathrm{D}t} & = & h, \quad \text{with} \quad s(\mathbf{x}, 0) = 0, \end{array} \right. \tag{4}$$

whose unique solution is noted $H(\mathbf{x}, t)$ (see remark 2). Then, noting $\boldsymbol{\omega}^\star = \mathbf{curl}\ \mathbf{v}^\star$

the vorticity perturbation, we rewrite (3) in the more convenient form

$$\frac{\partial \mathbf{v}^\star}{\partial t} + \boldsymbol{\nabla}(\mathbf{v}_0 \cdot \mathbf{v}^\star) + \boldsymbol{\omega}_0 \times \mathbf{v}^\star + \boldsymbol{\omega}^\star \times \mathbf{v}_0 + \boldsymbol{\nabla}\left(\frac{p}{\rho_0}\right) = \mathbf{g}, \tag{5a}$$

$$\frac{\mathrm{D}}{\mathrm{D}t}\left(\frac{p}{\rho_0 c_0^2}\right) + \frac{1}{\rho_0}\mathrm{div}(\rho_0 \mathbf{v}) = -f, \tag{5b}$$

$$\mathbf{v}^\star = \mathbf{v} - \frac{H\mathbf{v}_0}{2c_p}, \tag{5c}$$

$$\mathbf{v}^\star(\mathbf{x}, 0) = 0 = \quad p(\mathbf{x}, 0) = s(\mathbf{x}, 0). \tag{5d}$$

with

$$\boldsymbol{\omega}_0 = \mathbf{curl}\ \mathbf{v}_0, \tag{6}$$

the vorticity of the carrier flow and where we have used the vector identity Eq. (31).

2.2. Goldstein's equation with general sources in a general flow. In this paragraph, we aim at obtaining the Goldstein equations from Eq. ((5a),(5b),(5c),(5d)), with a general flow ($\boldsymbol{\omega}_0 = \mathbf{0}$ or $\neq \mathbf{0}$) and general sources f and $\mathbf{g}$. The Helmholtz decomposition indicates that $\mathbf{g}$ can be written $\mathbf{g} = \boldsymbol{\nabla} g_1 + \mathbf{curl}\ \mathbf{g}_2$, with $\mathbf{g}_2 = \mathbf{0}$ if $\mathbf{curl}\ \mathbf{g} = \mathbf{0}$. In 3D, the condition $\mathrm{div}\mathbf{g}_2 = 0$ is added whereas in 2D, g_2 becomes a scalar. We will prove the theorem:

THEOREM 1. *Euler's Equations ((5a),(5b),(5c),(5d)) are equivalent to the generalized Goldstein equations*

$$\left\{ \begin{array}{rcl} \dfrac{D}{Dt}\left(\dfrac{1}{c_0^2}\dfrac{D\varphi}{Dt}\right) - \dfrac{1}{\rho_0} div\left[\rho_0(\boldsymbol{\nabla}\varphi + \boldsymbol{\xi})\right] & = & F + \dfrac{D}{Dt}\left(\dfrac{g_1}{c_0^2}\right), \\ \dfrac{D\boldsymbol{\xi}}{Dt} + (\boldsymbol{\xi}\cdot\boldsymbol{\nabla})\boldsymbol{v}_0 - \boldsymbol{\nabla}\varphi \times \boldsymbol{\omega}_0 & = & \boldsymbol{curl}\ \boldsymbol{g}_2, \end{array} \right. \tag{7}$$

where

$$F = f + \frac{\boldsymbol{v}_0 \cdot \boldsymbol{\nabla} H}{2c_p},$$

associated to the initial conditions $\varphi(\boldsymbol{x}, 0) = 0 = (\partial\varphi/\partial t)(\boldsymbol{x}, 0) = \boldsymbol{\xi}(\boldsymbol{x}, 0)$*, with*

$$\left\{ \begin{array}{rcl} \boldsymbol{v} & = & \boldsymbol{\nabla}\varphi + \boldsymbol{\xi} + \dfrac{H\boldsymbol{v}_0}{2c_p}, \\ p & = & \rho_0\left(g_1 - \dfrac{D\varphi}{Dt}\right). \end{array} \right. \tag{8}$$

Before proving this theorem, let us make some remarks.

REMARK 1.

- *If all the sources are vanished* $\boldsymbol{g} = 0 = f = h$ *and if* $\boldsymbol{\omega}_0 = \boldsymbol{0}$*, Eq. (7) and Eq. (8) degenerate to the result of Goldstein [15]:*

$$\left\{ \begin{array}{rcl} \dfrac{D}{Dt}\left(\dfrac{1}{c_0^2}\dfrac{D\varphi}{Dt}\right) & = & \dfrac{1}{\rho_0} div\left[\rho_0(\boldsymbol{\nabla}\varphi + \boldsymbol{\xi})\right], \\ \dfrac{D\boldsymbol{\xi}}{Dt} & = & -(\boldsymbol{\xi}\cdot\boldsymbol{\nabla})\boldsymbol{v}_0. \end{array} \right. \tag{9}$$

- *The definition usually used [15, 18, 20, 21], $p = -\rho_0 D\varphi/Dt$, is no longer valid if $g_1 \neq 0$ (see Eq. (8)).*
- *the "acoustical" part g_1 of the source $\boldsymbol{g}$ appears as a source term only in the equation for the acoustic field φ. In a same way the "hydrodynamic" part $\boldsymbol{g}_2$ of the source $\boldsymbol{g}$ appears as a source term only in the equation for the hydrodynamic field $\boldsymbol{\xi}$.*
- *the decomposition of the velocity in Eq. (8) is not a Helmholtz decomposition since we have not imposed $\mathrm{div}\left(\boldsymbol{\xi} + \dfrac{H\boldsymbol{v}_0}{2c_p}\right) = 0$. In fact in practice this quantity is not found to be equal to zero and it happens that the Helmholtz decomposition is not well-adapted to aeroacoustics. We have chosen to use the Goldstein's decomposition $\boldsymbol{v}^\star = \boldsymbol{\nabla}\varphi + \boldsymbol{\xi}$, but an alternative is to use Clebsch potentials [16].*

Proof. It is straightforward to check that if φ and $\boldsymbol{\xi}$ are solutions of the coupled system of Goldstein's equations (7), then $p = \rho_0(g_1 - \mathrm{D}\varphi/\mathrm{D}t)$ and $\mathbf{v}^\star = \boldsymbol{\nabla}\varphi + \boldsymbol{\xi}$ are solutions of Eq. ((5a),(5b),(5c),(5d)). It has been already done without any source term, for isentropic perturbations ($s = 0$) [17, 18, 19, 20] or for general perturbations in a cylindrical geometry [21].

To prove the converse implication, that a solution of Euler's equations is a solution of Goldstein's equations, is more complicated and has never been done in the general case. A first difficulty is to define uniquely the Goldstein unknowns $(\varphi, \boldsymbol{\xi})$ from the Euler unknowns $(p, \mathbf{v}^\star)$. It has been done only for a potential flow and with incident fields as source terms [15]. To extend the results to a vortical flow and to the presence of sources, first we define φ, starting from (8) with the initial condition $\varphi(\mathbf{x}, 0) = 0$ (see remark 2). Then we deduce $\boldsymbol{\xi}$. More explicitly we use the relations

$$\left\{ \begin{array}{rcl} \dfrac{\mathrm{D}\varphi}{\mathrm{D}t} & = & g_1 - \dfrac{p}{\rho_0}, \quad \text{with } \varphi(\mathbf{x}, 0) = 0, \\ \boldsymbol{\xi} & = & \mathbf{v}^\star - \boldsymbol{\nabla}\varphi, \end{array} \right. \tag{10}$$

to define the Goldstein's unknowns $(\varphi, \boldsymbol{\xi})$.

Applying the change of unknowns Eq. (10), the mass conservation equation (5b) leads to

$$\frac{\mathrm{D}}{\mathrm{D}t}\left(\frac{1}{c_0^2}\frac{\mathrm{D}\varphi}{\mathrm{D}t}\right) = \frac{1}{\rho_0}\mathrm{div}[\rho_0(\boldsymbol{\nabla}\varphi + \boldsymbol{\xi})] + f + \frac{\mathrm{D}}{\mathrm{D}t}\left(\frac{g_1}{c_0^2}\right) + \frac{\mathbf{v}_0 \cdot \boldsymbol{\nabla}H}{2c_p}. \tag{11}$$

Moreover, using $\boldsymbol{\omega}^\star = \mathbf{curl}\ \boldsymbol{\xi}$, deduced form Eq. (10), (5a) leads to

$$\boldsymbol{\nabla}\left(\frac{\partial\varphi}{\partial t} + \mathbf{v}_0 \cdot \mathbf{v}^\star + g_1 - \frac{D\varphi}{Dt}\right) + \frac{\partial\boldsymbol{\xi}}{\partial t} + \boldsymbol{\omega}_0 \times \mathbf{v}^\star + \mathbf{curl}\ \boldsymbol{\xi} \times \mathbf{v}_0 = \mathbf{g},$$

which simplifies in:

$$\boldsymbol{\nabla}\left(\mathbf{v}_0 \cdot \boldsymbol{\xi}\right) + \frac{\partial\boldsymbol{\xi}}{\partial t} + \boldsymbol{\omega}_0 \times (\boldsymbol{\nabla}\varphi + \boldsymbol{\xi}) + \mathbf{curl}\ \boldsymbol{\xi} \times \mathbf{v}_0 = \mathbf{curl}\ \mathbf{g}_2.$$

Finally using once again Eq. (31) is obtained the hydrodynamic equation

$$\frac{\mathrm{D}\boldsymbol{\xi}}{\mathrm{D}t} = \boldsymbol{\nabla}\varphi \times \boldsymbol{\omega}_0 - (\boldsymbol{\xi} \cdot \boldsymbol{\nabla})\mathbf{v}_0 + \mathbf{curl}\ \mathbf{g}_2. \tag{12}$$

∎

REMARK 2. *An efficient method to solve the first equation of (10) or to solve Eq. (4) is to use a change of variable in order to get a family of ordinary differential equations along the streamlines of the flow. For instance, for a parallel shear flow* $\boldsymbol{v}_0(\boldsymbol{x}) = v_0(y)\boldsymbol{e}_x$ *with* $\boldsymbol{x} = (x, y, z)$*, the streamlines are the lines* $y = cste$ *and* $z = cste$ *and we get the explicit unique solutions:*

$$\varphi(\boldsymbol{x}, t) = \int_0^t \zeta[x - v_0(y)(t-u), y, z, u]\, du \quad where \quad \zeta(\boldsymbol{x}, t) = g_1(\boldsymbol{x}, t) - \frac{p(\boldsymbol{x}, t)}{\rho_0(\boldsymbol{x})},$$

$$H(\boldsymbol{x}, t) = \int_0^t h[x - v_0(y)(t-u), y, z, u]\, du.$$

2.3. General expression of the hydrodynamic unknown. The perturbation φ is governed by a classical convected wave-like equation (7), with source terms. The main difficulty is to determine $\boldsymbol{\xi}$, which satisfies a less classical transport-like equation. However there is a simplification: it is possible to find a simple expression of $\boldsymbol{\xi}$ which in particular predicts where $\boldsymbol{\xi}$ vanishes. We present now the derivation of such expression.

In the case of a potential flow $\boldsymbol{\omega}_0 = \mathbf{0}$ and of potential sources $\mathbf{g}_2 = \mathbf{0}$,it is easy to get from Eq. (12) that $\boldsymbol{\xi} = \mathbf{0}$ and Goldstein's equations (7) reduce to the potential model (Eq. (1) with the addition of source terms). In the general case of a non-potential flow in presence of non-potential sources, $\boldsymbol{\xi} \neq \mathbf{0}$ but a simple expression of $\boldsymbol{\xi}$ can also be obtained. Indeed Eq. (12) may be written

$$\frac{\mathrm{D}\boldsymbol{\xi}}{\mathrm{D}t} + (\boldsymbol{\xi} \cdot \boldsymbol{\nabla})\mathbf{v}_0 = \boldsymbol{\nabla}\varphi \times \boldsymbol{\omega}_0 + \mathbf{curl}\ \mathbf{g}_2. \tag{13}$$

This means that $\boldsymbol{\xi}$ is induced by two different sources: the coupling between acoustic perturbations $\boldsymbol{\nabla}\varphi$ and the flow vorticity $\boldsymbol{\omega}_0$ and the vorticity source term $\mathbf{curl}\ \mathbf{g}_2$. More precisely we will prove the following theorem:

THEOREM 2. *The general solution of Eq. (13) is*

$$\boldsymbol{\xi} = \boldsymbol{u} \times \boldsymbol{\omega}_0 + \boldsymbol{\sigma}, \tag{14}$$

where $\boldsymbol{u}$ *is the displacement perturbation and where* $\boldsymbol{\sigma}(\boldsymbol{g}_2)$ *is a term only due to the hydrodynamic source* $\boldsymbol{g}_2$ *(or equivalently to* $\boldsymbol{curl\ g}$*).*

$\mathbf{u}$ is defined from the velocity through (see [11])

$$\mathbf{v}^\star = \frac{\mathrm{D}\mathbf{u}}{\mathrm{D}t} - (\mathbf{u} \cdot \boldsymbol{\nabla})\mathbf{v}_0, \tag{15}$$

with the initial condition $\mathbf{u}(\mathbf{x}, 0) = \mathbf{0}$. To prove the Theorem 2 and the decomposition (14), we introduce the temporary unknown

$$\tilde{\boldsymbol{\xi}} = \mathbf{u} \times \boldsymbol{\omega}_0, \tag{16}$$

and we prove first the following lemma:

LEMMA 3. *The quantity* $\tilde{\boldsymbol{\xi}}$ *defined in Eq. (16) satisfies the following equation*

$$\frac{D\tilde{\boldsymbol{\xi}}}{Dt} = (\boldsymbol{v}^\star - \tilde{\boldsymbol{\xi}}) \times \boldsymbol{\omega}_0 - (\tilde{\boldsymbol{\xi}} \cdot \boldsymbol{\nabla})\boldsymbol{v}_0. \tag{17}$$

Note that this is simply a vectorial relation, which has nothing to do with the problems satisfied by $\mathbf{u}$ and $\mathbf{v}^\star$. We give the proof in the Appendix A.

Note that since $\boldsymbol{\nabla}\varphi = \mathbf{v}^\star - \boldsymbol{\xi}$, $\boldsymbol{\xi}$ in Eq. (12) with $\mathbf{curl}\ \mathbf{g}_2 = \mathbf{0}$ satisfies the same equation than $\tilde{\boldsymbol{\xi}}$ in Eq. (17). Thanks to this remark, from Eq. (12) and Eq. (17) we deduce that $\boldsymbol{\zeta} = \boldsymbol{\xi} - \tilde{\boldsymbol{\xi}}$ satisfies

$$\frac{\mathrm{D}\boldsymbol{\zeta}}{\mathrm{D}t} = -\boldsymbol{\zeta} \times \boldsymbol{\omega}_0 - (\boldsymbol{\zeta} \cdot \boldsymbol{\nabla})\mathbf{v}_0 + \mathbf{curl}\ \mathbf{g}_2, \tag{18}$$

with $\boldsymbol{\zeta}(\mathbf{x}, 0) = \mathbf{0}$.

We can now prove the Theorem 2 by solving Eq. (18), the solution depending of the value of the source term:

- if $\mathbf{curl}\ \mathbf{g}_2 = \mathbf{0}$, then the solution of Eq. (18) is zero (and thus $\boldsymbol{\xi} = \mathbf{u} \times \boldsymbol{\omega}_0$), since, it is easy to get that

$$\frac{d\mathcal{E}}{dt} \leq 2\left(\|\boldsymbol{\omega}_0\| + \|\boldsymbol{\nabla}\mathbf{v}_0\|\right)\mathcal{E},$$

  where $\mathcal{E} = \displaystyle\int_\Omega \frac{\rho_0}{2}\left|\boldsymbol{\zeta}\right|^2 d\mathbf{x}$. Since $\mathcal{E}(t=0) = 0$, we deduce thanks to Gronwall lemma that $\boldsymbol{\xi} = \tilde{\boldsymbol{\xi}}$ at any time.
- if $\mathbf{curl}\ \mathbf{g}_2 \neq \mathbf{0}$, if we note $\boldsymbol{\sigma}(\mathbf{g}_2)$ the unique solution (see the previous item for the homogeneous problem) of Eq. (18), then $\boldsymbol{\xi} = \tilde{\boldsymbol{\xi}} + \boldsymbol{\sigma}$.

REMARK 3. *In the case $\boldsymbol{g} = \boldsymbol{0}$ and for homentropic perturbations $s = 0$, the first part $\boldsymbol{\xi} = \boldsymbol{u} \times \boldsymbol{\omega}_0$ has already been found [16] whereas Goldstein [15], considering the case $\boldsymbol{\omega}_0 = \boldsymbol{0}$ but with an incident field, acting like a source term $\boldsymbol{curl}\ \boldsymbol{g} \neq \boldsymbol{0}$, found the second part $\boldsymbol{\xi} = \boldsymbol{\sigma}$.*

3. Numerical experiments.

To illustrate the superiority of the Goldstein equations with respect to the potential model (1), we will now solve in the time harmonic regime the radiation problem defined by equations (7). We use a Finite Element method, which, contrary to a Finite Differences method, has the main advantage to be well suitable for unstructured meshes, adapted to complex geometries. We will restrict to the 2D case.

3.1. Acoustic radiation in a parallel shear flow.

We start by considering the simple case of a shear flow for two reasons. First it is a validation case because for such flow, the link between different alternative models is simple. Second it is a simple way to control the vorticity of the carrier flow (it is the derivative of the velocity profile) and thus to quantify the domain of validity of the potential model Eq. (1).

3.1.1. Numerical scheme.

Let us consider a two dimensional shear flow in $\mathbb{R}^2$

$$\mathbf{v}_0(x, y) = v_0(y)\mathbf{e}_x, \tag{19}$$

with a velocity v_0 continuously differentiable on $\mathbb{R}$. We impose an homentropic flow ($s_0 = cst$) and we get from the Linearized Euler Equations that the density ρ_0, the pressure p_0 and the sound velocity c_0 are constant. We suppose the flow subsonic $|\mathbf{v}_0| < c_0$ and we introduce the Mach number $M_0(y) = v_0(y)/c_0$. We consider harmonic noise sources $F(\mathbf{x})e^{-i\omega t}$ and $\mathbf{g}(\mathbf{x})e^{-i\omega t}$ with the frequency ω and we solve (7) with (2) replaced by

$$\frac{\mathrm{D}}{\mathrm{D}t} = -i\omega + \mathbf{v}_0 \cdot \boldsymbol{\nabla}.$$

Time harmonic regime seems easier to solve than transient regime since the time variable has disappeared, but it introduces an extra major difficulty when solving numerically a radiation problem: to consider a bounded domain, we have to define some well-suited radiation conditions. In this aim, following the treatment of Galbrun's equation [11], we surround the computational domain with perfectly matched layers (PMLs) [31, 32]. The computational domain, schematized on Fig. 1, is $\Omega = \Omega_L \cup \Omega_b$ where $\Omega_b =]x_m, x_p[\times]0, h[$ is the physical bounded domain containing at least the sources, $\Omega =]x_m - L_1, x_p + L_1[\times] - L_2, h + L_2[$ is the computational domain and $\Omega_L = \Omega \backslash \Omega_b$ is the PML domain. The velocity v_0 is supposed uniform outside $[0, h]$ in order to get no reflected waves from the domain outside Ω_b (otherwise the PMLs could not be introduced). The introduction of PMLs corresponds to define the scale changes

$$\forall (x,y) \in \Omega, \quad \begin{cases} \dfrac{\partial}{\partial x} \to \check{\alpha}_1(x) \dfrac{\partial}{\partial x} \\ \dfrac{\partial}{\partial y} \to \check{\alpha}_2(y) \dfrac{\partial}{\partial y} \end{cases}$$

where the piecewise functions $\check{\alpha}_i$ are defined by

$$\check{\alpha}_1(x) = \begin{cases} 1 & \text{if} \quad x \in]x_m, x_p[, \\ \alpha \in \mathbb{C} & \text{otherwise.} \end{cases} \qquad \check{\alpha}_2(y) = \begin{cases} 1 & \text{if} \quad y \in]0, h[, \\ \alpha \in \mathbb{C} & \text{otherwise.} \end{cases}$$

The complex number α in the PMLs is chosen such that [11]

$$Re(\alpha) > 0 \quad \text{and} \quad Im(\alpha) < 0. \tag{20}$$

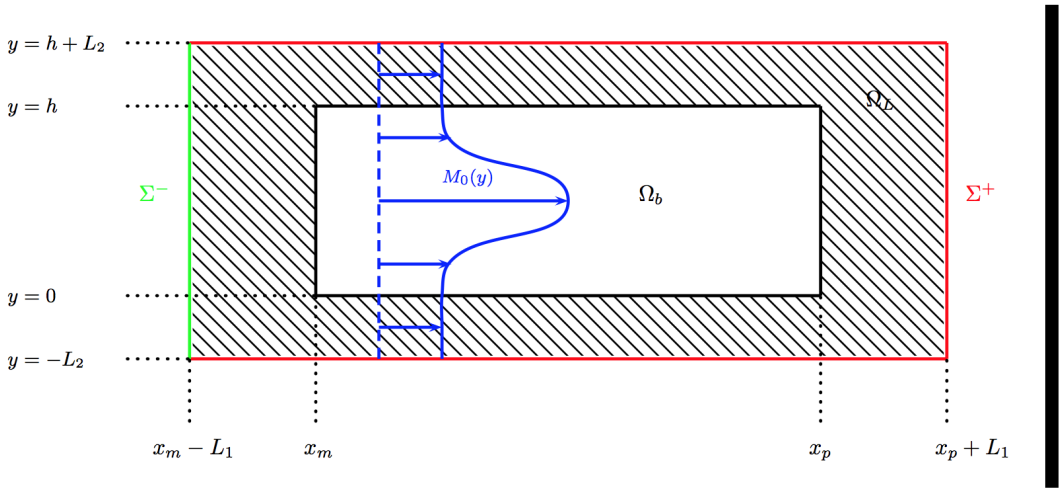

FIG. 1. *Description of the two dimensional problem with PMLs*

The purpose of these PMLs is to let the outgoing waves exit Ω_b and to suppress any reflected wave from the borders of Ω_b, in order to simulate the propagation without boundaries. The outgoing solution is selected by the PMLs by setting the boundary

conditions $\varphi = 0$ on $\Sigma^{\pm}$ and $\boldsymbol{\xi} = \mathbf{0}$ on Σ^{-} (since $\boldsymbol{\xi}$ satisfies a transport equation, it just needs to be set upstream [11]).

The Goldstein equations, in time harmonic regime, with PMLs and in a parallel shear flow become

$$\left\{\begin{array}{rcl} \mathrm{D}_\alpha^2\varphi & = & \mathrm{div}_\alpha(\boldsymbol{\nabla}_\alpha\varphi + \boldsymbol{\xi}) + F + \mathrm{D}_\alpha\left(\dfrac{g_1}{c_0}\right), \\ \mathrm{D}_\alpha\xi_x & = & -M_0'(y)\left(\check{\alpha}_2\dfrac{\partial\varphi}{\partial y} + \xi_y\right) + \check{\alpha}_2\dfrac{\partial g_2}{\partial y}, \\ \mathrm{D}_\alpha\xi_y & = & M_0'(y)\check{\alpha}_1\dfrac{\partial\varphi}{\partial x} - \check{\alpha}_1\dfrac{\partial g_2}{\partial x}, \end{array}\right. \tag{21}$$

where $\mathrm{D}_\alpha = -ik + M_0(y)\check{\alpha}_1\partial/\partial x$ with $k = \omega/c_0$. Thanks to the PMLs, we can prove that problem (21) is of Fredholm type, which in particular ensures the convergence of a Finite Element approximation of the solution (outside an eventual set of discrete resonance frequencies). More precisely we can prove that (the demonstration is rather technical and not given here):

THEOREM 4. *Problem (21) is of Fredholm type if*

$$\min\left[\Re e\,(\alpha)\,(1-s_0^2), \Re e\left(\frac{1}{\alpha}\right)\right] - s_1 C_{\alpha,\Omega} > 0, \tag{22}$$

where $s_0 = \max\limits_{y\in[0,h]}|M_0(y)|$, $s_1 = \max\limits_{y\in[0,h]}\left|\dfrac{M_0'(y)}{M_0(y)}\right|$ *and* $C_{\alpha,\Omega}$ *is a constant depending of the PML parameter and of the geometry of* Ω.

REMARK 4. *Note that thanks to Eq. (20), both* $\Re e\,(\alpha)$ *and* $\Re e\,(1/\alpha)$ *are positive. Therefore the theorem requires that* $s_0 < 1$ *(subsonic flow) and that* s_1 *is small enough (low shear flow). It is known that an incompressible shear flow with an inflection point in the velocity profile may be unstable if the slope is large enough. The condition* s_1 *small is certainly linked to this instability, although the condition* $M_0'' = 0$ *does not appear explicitly in the condition (22). The stability of compressible shear flows has been less studied, results can be found in the low frequency limit [33], but no explicit results on the influence of* $\max_{y\in[0,h]}|M_0'|$ *are given is this reference.*

REMARK 5. *The condition (22) is impossible to fulfill if* M_0 *vanishes, but we have found an alternative condition that replaces the condition (22) for vanishing or even low Mach number values. If* $M_0(y_0) = 0$*, then let us introduce the small layer* $y \in [y_0 - \varepsilon, y_0 + \varepsilon]$ *where* ε *is chosen such that* M_0 *is small in this layer. Then the radiation problem (21) is found to be globally well posed if it is well-posed both*

- *in the "low Mach" layer* $y \in [y_0 - \varepsilon, y_0 + \varepsilon]$*, which is the case under the condition:*

$$\min\left[Re\,(\alpha)\,(1-s_0^2), Re\left(\frac{1}{\alpha}\right)\right] - \frac{\max_{y\in[y_0-\varepsilon,y_0+\varepsilon]}|M_0'(y)|}{k} > 0, \tag{23}$$

- *outside the "low Mach" layers, which is the case if the condition (22) is satisfied by* $s_1 = \max\limits_{y\notin[y_0-\varepsilon,y_0+\varepsilon]}\left|\dfrac{M_0'(y)}{M_0(y)}\right|$.

REMARK 6. *Conditions (22) and (23) are sufficient conditions to get a well-posed radiation problem. In practice, the numerical method is stable for less restrictive conditions.*

A numerical method for solving the Galbrun Equation has been developed in the case of shear flows [34, 35], and then extended to slow [36] and general flows [11]. This numerical approach relies on a Finite Element method coupling continuous and Discontinuous elements [37, 38, 39], these latter leading to a stable method to deal with harmonic transport problems. The numerical scheme to solve Goldstein's equations is not new, we have adapted the numerical scheme developped to solve Galbrun's equation. Here we just sum up the numerical approach, for more details, see [11]. To solve the Goldstein equations, we couple two Finite Element schemes: the potential equation of (21) is discretized with Lagrange Finite Elements whereas the hydrodynamic equations of (21) are discretized with Discontinuous Galerkin Elements. Both quantities are discretized on the same mesh with around 70 000 nodes. They are determined conjointly and time calculations are of the order of a few minutes.

3.1.2. Parameters for the numerical simulations. We work with variables and unknowns without dimension which leads to $\rho_0 = c_0 = 1$. In most of the numerical results, we consider a jet flow of Mach number given by

$$M_0(y) = M_\infty + \mu \exp\left(-\frac{y^2}{R^2}\right), \tag{24}$$

where μ, M_∞ and R are parameters. We consider first $F = 0$ in Eq. (21), $g_2 = 0$ (thus the hydrodynamic field $\boldsymbol{\xi}$ is equal to $\mathbf{u} \times \boldsymbol{\omega}_0$, see Eq. (14)) and two types of acoustic sources g_1, such that $\boldsymbol{\nabla} g_1$ is a dipolar or a quadripolar source:

$$\begin{aligned} g_1^*(x,y) &= \exp\left(-\frac{(x-x_c)^2+(y-y_c)^2}{r_S^2}\right), \\ \widetilde{g}_1(x,y) &= \frac{(x-x_c)(y-y_c)}{r^2}\exp\left(-\frac{(x-x_c)^2+(y-y_c)^2}{r_S^2}\right). \end{aligned} \tag{25}$$

(x_c, y_c) is the center of the source and r_S is its characteristic radius. For simplicity we consider isentropic disturbances $s = 0$, which implies $\mathbf{v}^\star = \mathbf{v}$ in Eq. (3), and we will compare three models, where $\mathrm{D}/\mathrm{D}t = M_0(y)\partial/\partial x - ik$ with $k = \omega/c_0$:

- the potential model

$$\frac{\mathrm{D}^2\varphi}{\mathrm{D}t^2} = \mathrm{div}(\boldsymbol{\nabla}\varphi) + \frac{\mathrm{D}g_1}{\mathrm{D}t},$$

- the Goldstein model

$$\begin{cases} \dfrac{\mathrm{D}^2\varphi}{\mathrm{D}t^2} &= \mathrm{div}(\boldsymbol{\nabla}\varphi + \boldsymbol{\xi}) + \dfrac{\mathrm{D}g_1}{\mathrm{D}t}, \\ \dfrac{\mathrm{D}\boldsymbol{\xi}}{\mathrm{D}t} &= \boldsymbol{\nabla}\varphi \times \boldsymbol{\omega}_0 - (\boldsymbol{\xi}\cdot\boldsymbol{\nabla})\mathbf{M}_0, \end{cases} \tag{26}$$

  with $\boldsymbol{\omega}_0 = \mathbf{curl}\ \mathbf{M}_0$,

- the Galbrun model (see [12, 11])

$$\frac{\mathrm{D}^2\mathbf{u}}{\mathrm{D}t^2} - \boldsymbol{\nabla}(\boldsymbol{\nabla}\cdot\mathbf{u}) = \boldsymbol{\nabla} g_1. \tag{27}$$

Thanks to the introduction of the source term $\boldsymbol{\nabla} g_1$ in Eq. (27), it is possible to prove that Eq. (26) and Eq. (27) are equivalent. Our aim is to illustrate the efficiency of the Goldstein model. The Galbrun model is introduced as a reference method and the potential model is used for its simplicity. More precisely:

- Since the Galbrun model has been implemented and tested on many cases [11], it will be used to produce reference solutions to test the validity of the numerical resolution of the Goldstein equations. To compare the numerical results from the three models, we need to consider common quantities: the pressure and the velocity. These quantities are given by

$$p = g_1 - \frac{\mathrm{D}\varphi}{\mathrm{D}t} = -\mathrm{div}\ \mathbf{u} \quad \text{and} \quad \mathbf{v} = \boldsymbol{\nabla}\varphi + \boldsymbol{\xi} = \frac{\mathrm{D}\mathbf{u}}{\mathrm{D}t} - (\mathbf{u}\cdot\boldsymbol{\nabla})\mathbf{M}_0.$$

- The potential model is very attractive because its resolution is simple: only continuous Finite Element are required. Although it is not valid for non-potential flows, it can be solved for any flows and the comparison with Goldstein's model will indicate the importance of the induced error. The results will be presented first for low shear flows, for which the error when using the potential model is expected to be small, then for stronger shear flows and finally for a potential flow with an hydrodynamic source.

3.1.3. Comparisons for a low vorticity flow. First we consider a jet flow associated to a low vorticity $|\boldsymbol{\omega}_0|$, defined by $R = 0.35$, $M_\infty = 0.1$ and $\mu = 0.2$ in the domain $\Omega_b =]0,3[\times]-1,1[$. The source is g_1^* (see Eq. (25)) with $(x_c, y_c) = (1,0)$, $r_S = 0.05$ and $k = 12$. For small $|\boldsymbol{\omega}_0|$ values, $\boldsymbol{\xi} = \mathbf{u}\times\boldsymbol{\omega}_0$ is small and the potential model is expected to be a rather good approximation. More quantitatively, the term $\boldsymbol{\nabla}\varphi$ is dominant over the hydrodynamic term $\boldsymbol{\xi}$ in the acoustic velocity decomposition Eq. (10). Indeed the vorticity $\boldsymbol{\omega}_0 = -\mathrm{d}M_0/\mathrm{d}y\mathbf{e}_z$ is bounded by

$$\omega_0 \equiv |\boldsymbol{\omega}_0| = \frac{2\mu}{R^2} y \exp\left(-\frac{y^2}{R^2}\right) \leq \sqrt{\frac{2}{e}}\frac{\mu}{R}.$$

From the second equation of (26), we get the rough estimate $\omega|\boldsymbol{\xi}| \sim \omega_0|\boldsymbol{\nabla}\varphi|$ and therefore $|\boldsymbol{\xi}|/|\boldsymbol{\nabla}\varphi| \sim \omega_0/\omega \leq 0.04$.

On Fig. 2 and Fig. 3 are represented respectively the horizontal acoustic velocity and the pressure radiated by the source for the three models. The horizontal white lines delimit the area with a strong shear of the flow. We obtain very similar numerical

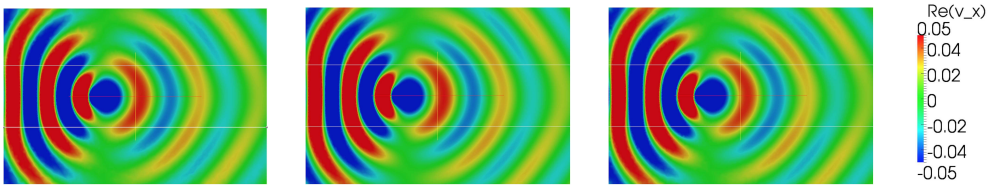

FIG. 2. *Real part of the velocity perturbation $Re(v_x)$ in a low shear jet flow Eq. (24) for Goldstein (left), Galbrun (center) and the potential model (right). The shear area is between the white lines. The source corresponds to the central disc. For such a low shear flow, the solutions of the three different equations are found very similar*

solutions, which confirms that the potential model may be used as a good approximation in this low shear case. Actually, there are small differences in the vorticity areas (between the white lines) on the acoustic velocity but no difference on the pressure. The impact of these differences on the far-fields is found very limited.

3.1.4. Comparisons for a larger vorticity flow. We consider now for the same geometry and the same source a jet flow with a stronger vorticity, $R = 0.15$ and

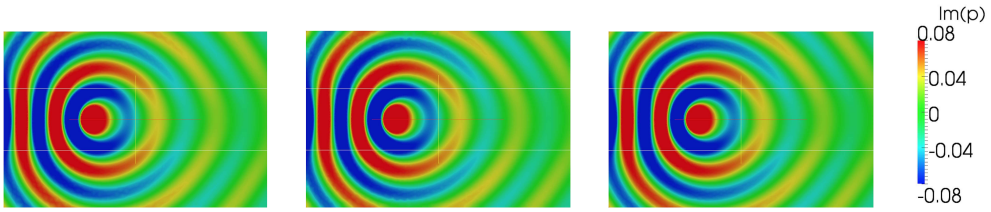

FIG. 3. *Imaginary part of the pressure perturbation $Im(p)$ for the same configuration than in Fig. 2 for: Goldstein (left), Galbrun (center) and the potential model (right). Since the pressure in not an hydrodynamic quantity, the three solutions are nearly the same.*

thus $|\boldsymbol{\xi}|/|\boldsymbol{\nabla}\varphi| \sim \omega_0/\omega \leq 0.1$, for which only the Goldstein and the Galbrun models are rigorously valid. We have checked that Goldstein's and Galbrun's models give the same results and we focus here on the comparison between Goldstein's and potential models: on Fig. 4 are represented $Re(\mathbf{v}_x)$ radiated by a source from the Goldstein model on the left and from the potential model on the right at $k = 8$. Differences between the two solutions, especially in the vorticity area (between the white lines, in the vicinity of $y = 0$), are observed. In particular the Goldstein equations are able to

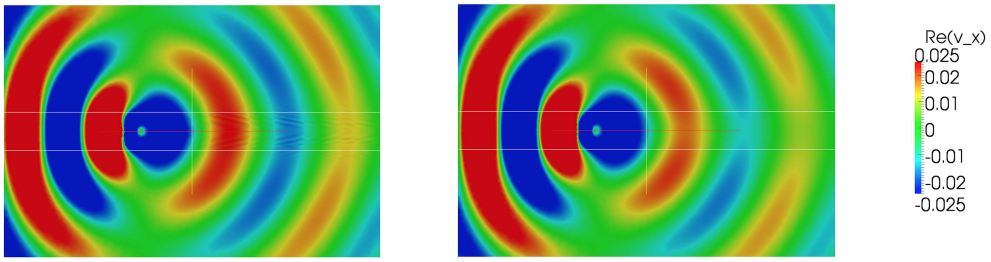

FIG. 4. *Real part of the velocity perturbation $Re(v_x)$ in a strong shear jet flow for Goldstein (left) and the potential model (right). Hydrodynamics patterns, appearing as inclined lines with a small wavelength, are forgotten by the potential model.*

capture the hydrodynamic phenomena, neglected by the potential model: oscillations of v_x (inclined lines of small wavelength downstream the source, due to oscillations of $\boldsymbol{\xi}$) are seen on Fig. 4 left part, as a result of the transport phenomenon (see [11]). Indeed the solution of $\mathrm{D}\boldsymbol{\xi}/\mathrm{D}t = 0$ is $\boldsymbol{\xi} = \mathcal{A}(y)\exp(ikx/M_0(y))$: for each y value, it corresponds to patterns moving at $M_0(y)$ with a wavelength $2\pi M_0(y)/k$.

In the previous example, the impact of neglecting $\boldsymbol{\xi}$ is found very limited: indeed, the radiated patterns for the Goldstein and potential models in Fig. 4 are very similar. This is because $|\boldsymbol{\xi}|/|\boldsymbol{\nabla}\varphi| \leq 0.1$. But in general it is important not to neglect hydrodynamic phenomena since strong differences in the far field can occur. Such differences are easier to see, considering a new geometry: we consider a larger domain $\Omega_b =]-3, 3[^2$, $k = 12$ and we place the quadripolar source $\widetilde{g}_1$ of Eq. (25) at $(x_c, y_c) = (-1, 1.5)$ with $r_S = 0.1$. The jet flow corresponds to $R = 0.1$, $M_\infty = 0$ and $\mu = 0.3$. The results obtained from the three models are presented on Fig. 5. The far fields obtained for the Goldstein and the Galbrun models are equivalent and both different from the result given by the potential flow model. The far field of the potential solution is clearly different downstream the source, in particular for the rays reflected by the jet core, highlighted by dashed lines.

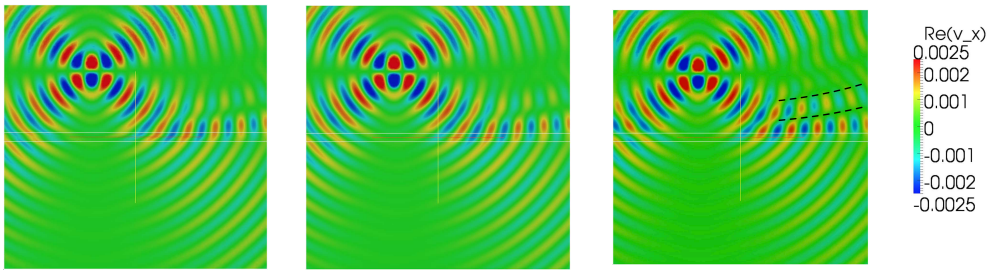

FIG. 5. *Real part of the velocity perturbation $Re(v_x)$ for the radiation of a quadripolar source for Goldstein (left), Galbrun (center) and the potential model (right). A large domain enables us to see the far field. The dashed black lines highlight the main differences between the potential model and the other models. In particular an extra reflected "ray", non physical, is obtained by the potential model.*

Finally, to illustrate the validity of the relation $\boldsymbol{\xi} = \mathbf{u} \times \boldsymbol{\omega}_0$ where $\mathbf{u}$ is the perturbation displacement, we consider on Fig. 6 the case $\Omega_b =]0,3[\times]-1,1[$, $k = 6$, the jet flow characterized by $R = 0.25$, $M_\infty = 0.2$, $\mu = 0.1$ and the source g_1^*, represented by a black circle. $Re(\xi_x)$ from the Goldstein equations and $Re((\mathbf{u}\times\boldsymbol{\omega}_0)_x)$

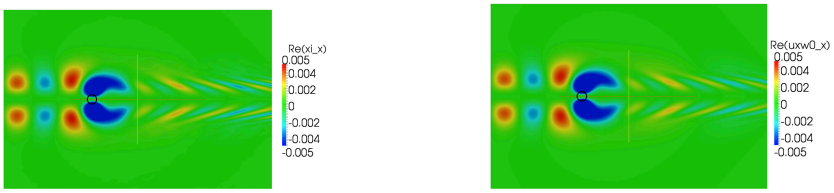

FIG. 6. *Validation of the relation $\boldsymbol{\xi} = \boldsymbol{u} \times \boldsymbol{\omega}_0$ for the radiation of a dipolar source, represented as a black circle, in a jet flow. We represent $Re(\xi_x)$ for Goldstein (left) and $Re((\boldsymbol{u} \times \boldsymbol{\omega}_0)_x)$ for Galbrun (right). ξ_x develops only in the shear flow areas. Note that ξ_x does not vanish upstream the source.*

from the Galbrun Equation are found exactly equal. Note that $\boldsymbol{\xi}$ is not only convected by the flow, it takes non zero values upstream the source. This is due to the fact that the acoustic field $\mathbf{u}$ is radiated in all directions by the source.

3.2. Case of a 2D flow. In this section, we extend our illustrations to non-shear flow and non-potential sources. We focus on Goldstein's configuration [15] and we consider a potential flow with a vortical source ($g_2 \neq 0$). We consider the flow around a circular obstacle of radius R, $\mathbf{M}_0(x,y) = \boldsymbol{\nabla}\varphi_0$ with

$$\varphi_0 = M_\infty \left(\frac{r}{R} + \frac{R}{r}\right)\cos\theta,$$

in polar coordinates ($x = r\cos\theta, y = r\sin\theta$). Such flow and source lead to the following equations:

$$\left\{\begin{array}{rcl} \dfrac{\mathrm{D}^2\varphi}{\mathrm{D}t^2} & = & \mathrm{div}(\boldsymbol{\nabla}\varphi + \boldsymbol{\xi}) + \dfrac{\mathrm{D}g_1}{\mathrm{D}t}, \\ \dfrac{\mathrm{D}\boldsymbol{\xi}}{\mathrm{D}t} & = & -(\boldsymbol{\xi}\cdot\boldsymbol{\nabla})\mathbf{M}_0 + \mathbf{curl}\ g_2, \end{array}\right.$$

with $\mathrm{D}/\mathrm{D}t = \mathbf{M}_0\cdot\nabla - ik$ and where we take $g_1 = g_1^* = g_2$ (see Eq. (25)). From

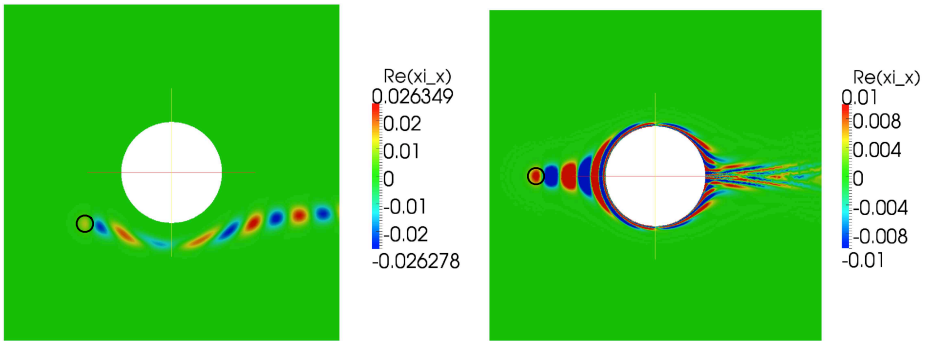

FIG. 7. *Radiation of a vortical source in the potential flow around a disc. Are represented $Re(\xi_x)$ obtained from the resolution of Goldstein's equations for two different positions of an hydrodynamic source, represented as a black circle. As expected, $Re(\xi_x)$ is convected along the flow streamlines. Note that the potential model neglects ξ_x (it assumes it is zero).*

Eq. (14), since for a potential flow $\mathbf{u}\times\boldsymbol{\omega}_0 = \mathbf{0}$, we have $\boldsymbol{\xi} = \boldsymbol{\sigma}$. On Fig. 7, for a flow coming horizontally from the left, is represented $\sigma_x = Re(\xi_x)$ in $\Omega_b =]-1,1[^2$, for $R = 0.3$, $M_\infty = 0.3$, $k = 6$ and for two different positions of the source. We see $\boldsymbol{\xi}$, created by the source whose location is indicated by a black circle, and following the flow streamlines. On Fig. 7 (left) the source is off-centered from the flow whereas on Fig. 7 (right) the source is centered on the stream line associated to a stop point on the disc. In the second case the pattern of $Re(\xi_x)$ is rather complex and behind the disc, the wavelength of $Re(\xi_x)$ is very small because the velocity is weak. Note that the potential model would ignore these patterns since this model consists in taking $\boldsymbol{\xi} = \mathbf{0}$ in the Goldstein equation and therefore the potential model is a bad approximation when g_2 is not small.

4. Concluding remarks. In order to study the acoustic radiation of a general source in a complex flow, we have derived the generalized Goldstein equations in the presence of a vortical flow and source terms. These equations extend the potential model, valid for potential flows, to general flows, by including a vector hydrodynamic field.

Firstly, by taking some acoustic and hydrodynamic source terms into account, we have proved that the Goldstein equations are equivalent to the Linearized Euler model. For source terms f and $\mathbf{g} = \boldsymbol{\nabla}g_1 + \mathbf{curl}\ \mathbf{g}_2$ introduced in Eq. (5a), we have established that the generalized Goldstein equations can be written (see Eq. (7)) in the following way:

$$\left\{\begin{array}{rcl} A\varphi + B\boldsymbol{\xi} & = & S, \\ C\boldsymbol{\xi} + \mathrm{D}\varphi & = & \mathbf{curl}\ \mathbf{g}_2. \end{array}\right.$$

The operators A, B, C and D are defined as:

$$\left\{\begin{array}{rcl} A\varphi & = & \dfrac{\mathrm{D}}{\mathrm{D}t}\left(\dfrac{1}{c_0^2}\dfrac{\mathrm{D}\varphi}{\mathrm{D}t}\right) - \dfrac{1}{\rho_0}\mathrm{div}\,[\rho_0 \boldsymbol{\nabla}\varphi)], \\ B\boldsymbol{\xi} & = & -\dfrac{1}{\rho_0}\mathrm{div}\,(\rho_0\boldsymbol{\xi}), \\ C\boldsymbol{\xi} & = & \dfrac{\mathrm{D}\boldsymbol{\xi}}{\mathrm{D}t} + (\boldsymbol{\xi}\cdot\boldsymbol{\nabla})\mathbf{v}_0, \\ D\varphi & = & -\boldsymbol{\nabla}\varphi\times\boldsymbol{\omega}_0. \end{array}\right.$$

We have introduced the general source term

$$S = f + \frac{\mathrm{D}}{\mathrm{D}t}\left(\frac{g_1}{c_0^2}\right) + \frac{\mathbf{v}_0\cdot\boldsymbol{\nabla}H}{2c_p},$$

where H denotes the entropic perturbation. Moreover the solution $\boldsymbol{\xi}$ of the hydrodynamic equation of Eq. (7) may be written in the form (Eq. (14)):

$$\boldsymbol{\xi} = \mathbf{u}\times\boldsymbol{\omega}_0 + \boldsymbol{\sigma}(\mathbf{g}_2),$$

where $\boldsymbol{\sigma}$ is the solution to (Eq. (18)):

$$\frac{\mathrm{D}\boldsymbol{\sigma}}{\mathrm{D}t} + (\boldsymbol{\sigma}\cdot\boldsymbol{\nabla})\mathbf{v}_0 + \boldsymbol{\sigma}\times\boldsymbol{\omega}_0 = \mathbf{curl}\ \mathbf{g}_2.$$

Our conclusions depend on the value of the vorticity of the flow $\boldsymbol{\omega}_0$ and of the value of $\mathbf{curl}\ \mathbf{g}$ in the momentum conservation law of Euler's equations. An overview of these conclusions is summarized in the following table:

	$\mathbf{curl}\ \mathbf{g} = 0$	$\mathbf{curl}\ \mathbf{g} \neq 0$
$\boldsymbol{\omega}_0 = 0$	$A\varphi = S$ $\boldsymbol{\xi} = \mathbf{0}$ Blokhintzev's model[4]	$A\varphi = S - B\boldsymbol{\sigma}$ $\boldsymbol{\xi} = \boldsymbol{\sigma}$ Goldstein's model[15]
$\boldsymbol{\omega}_0 \neq 0$	$A\varphi + B\boldsymbol{\xi} = S$ $C\boldsymbol{\xi} + D\varphi = \mathbf{0}$ $\boldsymbol{\xi} = \mathbf{u}\times\boldsymbol{\omega}_0$ Visser's model[16]	$A\varphi + B\boldsymbol{\xi} = S$ $C\boldsymbol{\xi} + D\varphi = \mathbf{curl}\ \mathbf{g}_2$ $\boldsymbol{\xi} = \mathbf{u}\times\boldsymbol{\omega}_0 + \boldsymbol{\sigma}$ New model

After the first theoretical section, we have presented a numerical method to solve the Goldstein equations in the time harmonic regime. PMLs have been introduced in order to bound the computational domain in the case of a two dimensional flow. The numerical method has been validated by a comparison with the Galbrun Equation and the importance of the hydrodynamic unknown has been emphasized by a comparison with the potential model.

A natural extension of this work is to consider more complicated boundary conditions than rigid boundaries, like impedance boundary conditions. Another perspective is to extend the numerical method to the 3D case. A possible strategy to decrease the computational cost, due to the introduction of many degrees of freedom by the Discontinuous Galerkin Element method, would be to compute φ and $\boldsymbol{\xi}$ on different meshes: $\boldsymbol{\xi}$ would be determined on a coarser mesh, since it is associated to small wavelengths, but on a mesh of small extension since only restricted to the vortical areas of the carrier flow.

Acknowledgments. The authors gratefully acknowledge the Agence Nationale de la Recherche (AEROSON project, ANR-09-BLAN-0068-02 program) for financial support.

Appendix A. Hydrodynamic field.

Here we prove the lemma 3: $\tilde{\boldsymbol{\xi}} = \mathbf{u} \times \boldsymbol{\omega}_0$ satisfies

$$\frac{\mathrm{D}\tilde{\boldsymbol{\xi}}}{\mathrm{D}t} = (\mathbf{v}^\star - \tilde{\boldsymbol{\xi}}) \times \boldsymbol{\omega}_0 - (\tilde{\boldsymbol{\xi}} \cdot \boldsymbol{\nabla})\mathbf{v}_0.$$

Proof. The carrier flow satisfies the Euler Equations:

$$\begin{cases} \mathrm{div}(\rho_0 \mathbf{v}_0) = 0, \\ \rho_0(\mathbf{v}_0 \cdot \boldsymbol{\nabla})\mathbf{v}_0 + \boldsymbol{\nabla} p_0 = 0, \end{cases} \tag{28}$$

associated to the state law of the fluid $p_0 = \nu(\rho_0)$, given by

$$\nu(\rho_0) = \kappa \rho_0^\gamma, \tag{29}$$

where κ is a constant.

First the usual vorticity equation for $\boldsymbol{\omega}_0$ is recovered, by writing the second equation of (28), using Eq. (29), in the form

$$\boldsymbol{\nabla}\left(\frac{|\mathbf{v}_0|^2}{2}\right) + \boldsymbol{\omega}_0 \times \mathbf{v}_0 + \boldsymbol{\nabla}\left(\frac{\gamma}{\gamma - 1}\frac{p_0}{\rho_0}\right) = \mathbf{0}, \tag{30}$$

where we have used the vector identity

$$(\mathbf{a} \cdot \boldsymbol{\nabla})\mathbf{b} + (\mathbf{b} \cdot \boldsymbol{\nabla})\mathbf{a} = \boldsymbol{\nabla}(\mathbf{a} \cdot \mathbf{b}) + (\boldsymbol{\nabla} \times \mathbf{a}) \times \mathbf{b} + (\boldsymbol{\nabla} \times \mathbf{b}) \times \mathbf{a}, \tag{31}$$

with $\mathbf{a} = \mathbf{b} = \mathbf{v}_0$. Taking the curl of (30)leads to:

$$\frac{\mathrm{D}\boldsymbol{\omega}_0}{\mathrm{D}t} = (\boldsymbol{\omega}_0 \cdot \boldsymbol{\nabla})\mathbf{v}_0 - (\mathrm{div}\mathbf{v}_0)\boldsymbol{\omega}_0, \tag{32}$$

(the flow is stationary and thus $\mathrm{D}/\mathrm{D}t = \mathbf{v}_0 \cdot \boldsymbol{\nabla}$). Using the relations (15) and (32), we get (it is also Eq. (52) of [16])

$$\frac{\mathrm{D}(\mathbf{u} \times \boldsymbol{\omega}_0)}{\mathrm{D}t} = \mathbf{v}^\star \times \boldsymbol{\omega}_0 + \underbrace{[(\mathbf{u} \cdot \boldsymbol{\nabla})\mathbf{v}_0] \times \boldsymbol{\omega}_0 + \mathbf{u} \times [(\boldsymbol{\omega}_0 \cdot \boldsymbol{\nabla})\mathbf{v}_0] - (\mathrm{div}\mathbf{v}_0)(\mathbf{u} \times \boldsymbol{\omega}_0)}_{= \widetilde{\boldsymbol{\nabla}}(\mathbf{u} \cdot (\mathbf{v}_0 \times \boldsymbol{\omega}_0))} \tag{33}$$

in which we have used $\widetilde{\boldsymbol{\nabla}}$, the nabla operator applying only on $\mathbf{v}_0$ (while $\mathbf{u}$ and $\boldsymbol{\omega}_0$ are considered constant)(see [16]). Therefore we get

$$\frac{\mathrm{D}\tilde{\boldsymbol{\xi}}}{\mathrm{D}t} = \mathbf{v}^\star \times \boldsymbol{\omega}_0 - \widetilde{\boldsymbol{\nabla}}(\mathbf{v}_0 \cdot \tilde{\boldsymbol{\xi}}).$$

The vector identity (31), valid also for the operator $\widetilde{\boldsymbol{\nabla}}$, applied to $\tilde{\boldsymbol{\xi}}$ and $\mathbf{v}_0$ leads us to the result of the lemma. ∎

REFERENCES

[1] L. Ting and M. J. Miksis, *On vortical flow and sound generation*, SIAM Journal on Applied Mathematics 50(2), 521-536 (1990).

[2] L. Ting and O. M. Knio, *Vortical flow outside a sphere and sound generation*, SIAM Journal on Applied Mathematics 57(4), 972-981 (1997).

[3] A. S. Bonnet-Ben Dhia, L. Dahi, E. Lunéville and V. Pagneux, *Acoustic diffraction by a plate in a uniform flow*, Mathematical Models and Methods in Applied Sciences 12(05), 625-647 (2002).

[4] D. Blokhintzev, *The propagation of sound in an inhomogeneous and moving medium I.*, J. Acoust. Soc. Am. **18**(2), 322-328 (1946)

[5] A. D. Pierce, *Wave equation for sound in fluids with unsteady inhomogeneous flow*, J. Acoust. Soc. Am. **87**(6), 2292-2299 (1990)

[6] J. P. Coyette, *Manuel théorique ACTRAN*, Free Field Technologies, Louvain-la-Neuve, Belgique (2001)

[7] S. Duprey, *Etude mathématique et numérique de la propagation acoustique d'un turboréacteur*, Thèse de Doctorat de l'Université Henry Poincaré-Nancy 1 (2006)

[8] W. Eversman, *The Boundary condition at an Impedance Wall in a Non-Uniform Duct with Potential Mean Flow*, J. Acoust. Soc. Am. **246**(1), 63-69 (2001)

[9] Gabard, G., and Brambley, E. J., *A full discrete dispersion analysis of time-domain simulations of acoustic liners with flow*, Journal of Computational Physics 273, 310-326 (2014).

[10] S. W. Rienstra and W. Eversman, *A numerical comparison between multiple-scales and finite-element solution for sound propagation in lined flow ducts*, Journal of Fluid Mechanics **437**, 367-384 (2001)

[11] A. S. Bonnet-Ben Dhia, J. F. Mercier, F. Millot, S. Pernet and E. Peynaud, *Time-Harmonic Acoustic Scattering in a Complex Flow: A Full Coupling Between Acoustics and Hydrodynamics*, Commun. Comput. Phys. **11**(2), 555-572 (2012)

[12] H. Galbrun, *Propagation d'une onde sonore dans l'atmosphère terrestre et théorie des zones de silence*, Gauthier-Villars, Paris, France (1931)

[13] G. Gabard, R. J. Astley, and M. B. Tahar, *Stability and accuracy of finite element methods for flow acoustics: II. Two-dimensional effects*, International Journal for Numerical Methods in Engineering **63**, 974-987 (2005)

[14] F. Treyssede, G. Gabard, and M. B. Tahar, *A mixed finite element method for acoustic wave propagation in moving fluids based on an Eulerian-Lagrangian description*, J. Acoust. Soc. Am. **113**, 705-716 (2003)

[15] M. E. Goldstein, Unsteady vortical and entropic distortion of potential flows round arbitrary obstacles, *J. Fluid Mech.* **89**(3), 433-468 (1978)

[16] S. E. P. Bergliaffa, K. Hibberd, M. Stone and M. Visser, *Wave Equation for Sound in Fluids with Vorticity*, Physica D **191**, 121-136 (2004)

[17] V. V. Golubev and H.M. Atassi, *Sound propagation in an annular duct with mean potential swirling flow*, Journal of Sound and Vibration **198**(5), 601-616 (1996)

[18] V. V. Golubev and H. M. and Atassi, *Acoustic-vorticity waves in swirling flows*, J. Sound Vib. **209**(2), 203-222 (1998)

[19] A. J. Cooper and N. Peake, *Propagation of unsteady disturbances in a slowly varying duct with mean swirling flow*, Journal of Fluid Mechanics **445**, 207-234 (2001)

[20] O. V. Atassi, *Computing the sound power in non-uniform flow*, J. Sound Vib. **266**, 75-92 (2003)

[21] A. J. Cooper, *Effect of mean entropy on unsteady disturbance propagation in a slowly varying duct with mean swirling flow*, J. Sound Vib. **291**(3-5), 779-801 (2006)

[22] C. K. W. Tam and L. Auriault, *The wave modes in ducted swirling flows*, J. Fluid Mech. **371**, 1-20 (1998)

[23] C. J. Heaton and N. Peake, *Algebraic and exponential instability of inviscid swirling flow*, J. Fluid Mech. **565**, 279-318 (2006)

[24] C. Prax, F. Golanski and L. Nadal, *Control of the vorticity mode in the linearized Euler equations for hybrid aeroacoustic prediction*, J. Comput. Phys. **227**, 6044-6057 (2008)

[25] J. H. Seo and Y. J. Moon, *Linearized perturbed compressible equations for low Mach number aeroacoustics*, J. Comput. Phys. **218**, 702-719 (2006)

[26] F. Nataf, *A new approach to perfectly matched layers for the linearized Euler system*, J. Comput. Phys. **214**, 757-772 (2006)

[27] C. D. Munz, M. Dumbser and S. Roller, *Linearized acoustic perturbation equations for low Mach number flow with variable density and temperature*, Journal of Computational Physics 224(1), 352-364 (2007).

[28] W. A. Möhring, *A well proposed acoustic analogy based on a moving acoustic medium*, Proceedings 1st Aeroacoustic Workshop (in connection with the german research project SWING), Dresden (1999)

[29] C. Legendre, G. Lielens, J.-P. Coyette, *Sound Propagation in a sheared flow based on fluctuating total enthalpy as generalized acoustic variable*, Proceedings of of the Internoise 2012/ASME NCAD meeting, New York City, NY, USA (2012)
[30] D. C. Pridmore Brown, Sound propagation in a fluid flowing through an attenuating duct, *The Journal of the Acoustical Society of America* **30**(7), 670-670 (1958).
[31] E. Bécache, A.-S. Bonnet-Ben Dhia, and G. Legendre, *Perfectly matched layers for time-harmonic acoustics in the presence of a uniform flow*, SIAM J. Numer. Anal. **44**, 1191-1217 (2006)
[32] F. Q. Hu, *A perfectly matched layer absorbing boundary condition for linearized Euler equations with a non-uniform mean flow*, Journal of Computational Physics 208(2), 469-492 (2005).
[33] A.-S. Bonnet-BenDhia, M. Duruflé, P. Joly and L. Joubert, *Stability of Acoustic Propagation in a 2D Flow Duct: A Low Frequency Approach*, M3AS 21(5), 1121-1151 (2011)
[34] A. S. Bonnet-Ben Dhia, E. M. Duclairoir, G. Legendre and J. F. Mercier, *Time-harmonic acoustic propagation in the presence of a shear flow*, J. of Comp. and App. Math. **204**(2), 428-439 (2007)
[35] A. S. Bonnet-Ben Dhia, E. M. Duclairoir and J. F. Mercier, *Acoustic propagation in a flow: numerical simulation of the time-harmonic regime*, ESAIM Proceedings **22** (2007)
[36] A. S. Bonnet-Ben Dhia, J. F. Mercier, F. Millot and S. Pernet, *A low Mach model for time harmonic acoustics in arbitrary flows*, J. of Comp. and App. Math. **234**(6), 1868-1875 (2010)
[37] P. Delorme, P. Mazet, C. Peyret, and Y. Ventribout, *Computational Aeroacoustics applications based on a discontinuous Galerkin method*, Comptes rendus de mécanique **333**, 676-682 (2005)
[38] G. Gabard, *Discontinuous Galerkin methods with plane waves for time-harmonic problems*, Journal of Computational Physics **225**, 1961-1984 (2007)
[39] A. Ern and J.-L. Guermond, *Theory and practice of finite Element*, Applied Mathematical Sciences, Springer-Verlag, New York (2004)